PVTx Measurements for the R116 + CO_2 and R41 + CO_2 Systems. New Isochoric Apparatus

Giovanni Di Nicola,*,† Fabio Polonara,† Renato Ricci,‡ and Roman Stryjek§

Dipartimento di Energetica, Università Politecnica delle Marche, Ancona, Italy, DSSARR, Facoltà di Architettura, Università di Chieti, Chieti, Italy, and Institute of Physical Chemistry, Polish Academy of Sciences, Warsaw, Poland

A new isochoric apparatus was built for *PVTx* measurements in an extended temperature range from (210 to 360) K and at pressures up to 6.0 MPa. The setup was used to measure *PVTx* properties for the R116 + CO_2 and R41 + CO_2 systems, both in the two-phase and superheated vapor regions. The binary interaction parameters were derived from experimental data in the two-phase region by applying the flash method and the Carnahan−Starling−DeSantis equation of state (CSD EOS). The dew-point parameters were found by interpolating the $P-T$ isochoric sequences, again applying the CSD EOS. A composition-dependent mixing rule implemented in the CSD EOS improved the VLE data representation of both binary systems. The resulting binary interaction parameters were used for VLE parameter derivation. The superheated vapor region data were compared with those obtained by the Burnett method and using REFPROP 7.

Introduction

Hexafluoroethane (R116) has been studied as a constituent of the trifluoromethane (R23) + R116 azeotropic binary system, and its thermophysical properties in the gas phase have been the object of extensive study. Fluoromethane (R41) is used in the refrigeration industry as a constituent of several binary or ternary mixtures for replacing difluorochloromethane (R22). The main drawback of this refrigerant fluid lies in its flammability and far-from-negligible GWP, despite a zero ODP. In our search for fluids that are suitable for low-temperature refrigerant applications, we recently turned our attention to systems composed of hydrofluorocarbons (HFCs) and CO_2.[1,2]

In the present study, a redesigned isochoric setup was used to take measurements for both the two-phase and the superheated vapor regions, covering a wider temperature range (from 214 K to 360 K). The data in the two-phase region enable VLE parameters to be derived using a flash method with the Carnahan−Starling−De Santis[3] equation of state (CSD EOS). The dew point for each isochore was also found from the intersection of $P-T$ sequences and was used to derive the VLE parameters. The methods adopted have been described elsewhere.[4] The VLE parameters derived by the two methods were compared and revealed good consistency. A literature source was found for both the R116 + CO_2[5] and R41 + CO_2[6] binary systems.

Experimental section

Chemicals. Carbon dioxide was supplied by Sol SpA, and R41 and R116, by Lancaster Inc. Their purity was checked by gas chromatography using a thermal conductivity detector and was found to be 99.99%, 99.9%, and 99.7% in mass for CO_2, R41, and R116, respectively. All estimations were based on a peak area response.

* Corresponding author. E-mail: anfreddo@univpm.it. Tel:+39-0712204277. Fax:+39-0712804239.
† Università Politecnica delle Marche.
‡ Università di Chieti.
§ Polish Academy of Sciences.

Apparatus. The new experimental setup is illustrated in Figure 1. The main modification to the original apparatus concerned the twin thermostatic baths (7) filled with different silicone oils (Baysilone M10 and Baysilone M100, Bayer). After charging with the sample mixture, the setup can be operated over two temperature ranges (from (210 to 290) K and from (290 to 360) K) depending on which bath is used. The thermostatic baths are easy to move because of the new configuration of the system. The spherical cells and pressure transducer are immersed in one of the two thermostatic baths (7). An auxiliary thermostat (14) is used to reach below-ambient temperatures. The pressure and temperature data acquisition systems remained the same as in the previous apparatus[7,8] and will be only briefly described here.

An AISI 304 stainless steel spherical cell (1) containing the refrigerant sample is connected to a differential diaphragm pressure transducer (4) coupled to an electronic null indicator (5). In the new setup, the transducer and sphere were placed vertically, and a magnetic pump (3) for mixing the sample was connected to the sphere. A second spherical cell (2) was also connected and used for volume calibration. Because of the complex volume of the isochoric cell (1), its total volume (including the piping, the pressure transducer cavity, and magnetic pump volumes) was calibrated according to the classic Burnett calibration procedure, adopting helium as the reference fluid. After estimating the apparatus constant $N = (V_1 + V_2)/V_1$, we measured the auxiliary cell volume, V_2, by filling it with distilled water. Finally, the volume of the measurement cell, V_1, was found to be 273.5 ± 0.3 cm^3 at room temperature on the basis of several expansions from cell (1) to cell (2). A correction for the thermal expansion and pressure distortion of the isochoric cell was considered, as reported elsewhere.[8]

As in the past,[7,8] temperature is controlled by a PID device and measured with a calibrated resistance thermometer; the temperature's total uncertainty was found

10.1021/je049939g CCC: $30.25
Published on Web 02/05/2005

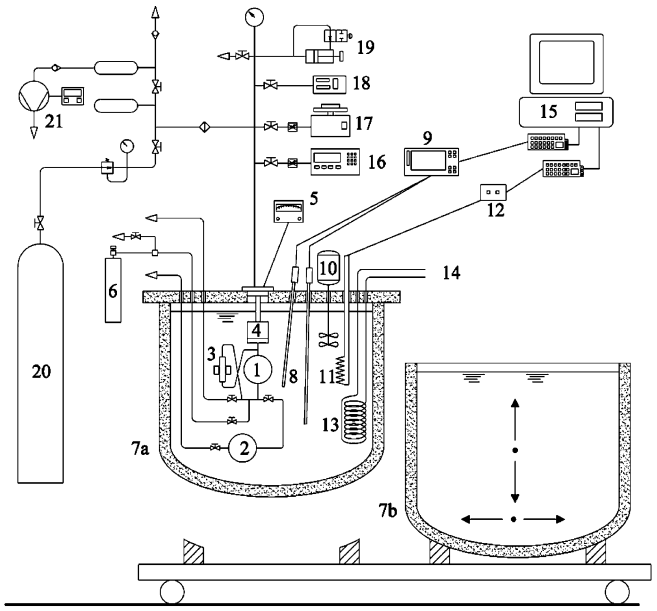

1	Constant volume spherical cell	12	Power system
2	Auxiliary cell	13	Cooling coil
3	Magnetic pump	14	Connections to auxiliary thermostatic bath
4	Differential pressure transducer	15	Acquisition system
5	Electronic null indicator	16	Bourdon gage
6	Charging system	17	Dead weight gage
7	Thermostatic baths	18	Vibrating cylinder pressure gage
8	Platinum thermo-resistances	19	Precision pressure controller
9	Thermometric bridge	20	Nitrogen reservoir
10	Stirrer	21	Vacuum pump system
11	Heater		

Figure 1. Schematic view of the experimental setup. Notation for symbols for the R116 (1) + CO_2 (2) system: ○, $x_1 = 0.2022$; □, $x_1 = 0.3964$; △, $x_1 = 0.5019$; ▽, $x_1 = 0.6396$; and ◇, $x_1 = 0.7702$. Notation for symbols for the R41 (1) + CO_2 (1) system: ○, $x_1 = 0.2431$; □, $x_1 = 0.3919$; △, $x_1 = 0.5034$; ▽, $x_1 = 0.6199$; and ◇, $x_1 = 0.7920$. x_1 denotes the mole fraction of the first compound.

to be lower than ±0.02 K. The uncertainty in the pressure measurements is due to the uncertainty of the transducer and null indicator system and the pressure gauges. The digital pressure indicator (Ruska, model 7000) has an uncertainty of ±0.003% of its full scale (kPa). The total uncertainty in the pressure measurement is also influenced by temperature fluctuations due to bath instability; it was found to be less than ±1 kPa.

Experimental Procedure. Mixtures were prepared using the gravimetric method. The experimental procedure has been described elsewhere.[4,9] The pure samples were first placed in different bottles, degassed to remove noncondensable gases and air, and weighed with an analytical balance (uncertainty ±0.3 mg). After evacuating the cell, we discharged the bottles into the cell immersed in the bath. At the end of this procedure, the bottles were weighed, and the mass of the charge was calculated from the difference between the two weights. The lost mass inside the duct was estimated and subtracted from the total mass of the charge. The uncertainty in molar composition measurements was estimated to be always lower than 0.1%.

Results and Discussion

The temperature and pressure ranges are shown in Table 1, along with the mixture's composition and the number of moles charged.

Analyzing the slope of each $T-P$ sequence, we attributed each experimental point either to the superheated or to the two-phase region. The experimental VLE data are given in Tables 2 and 3, and Tables 4 and 5 show the $PVTx$ measurements for R116 + CO_2 and R41 + CO_2, respectively. The number of data points belonging to each region is also included in Table 1. The data belonging to the two-phase region were fit by the Antoine equation, and the data in the superheated region were fit by a second-degree polynomial, taking temperature as the independent vari-

Table 1. Compositions of the Investigated Systems

R116 + CO_2

				N exptl points			dew point	
x_1	T range/K	P range/kPa	n/mol	2ph[a]	vap[a]	tot	T/K	P/kPa
0.2022	214−355	560−5610	0.65012	8	10	18	269.15	3343.0
0.3964	214−355	560−3160	0.33160	8	11	19	251.07	1848.7
0.5019	214−355	540−2800	0.29264	8	11	19	251.41	1675.8
0.6396	214−355	480−2230	0.22961	7	12	19	248.96	1333.9
0.7702	214−355	400−1870	0.19068	7	13	20	248.06	1125.9

R41 + CO_2

				N exptl points			dew point	
x_1	T range/K	P range/kPa	n/mol	2ph[a]	vap[a]	tot	T/K	P/kPa
0.2431	220−340	570−3070	0.34000	8	8	16	260.15	2071.8
0.3919	220−350	530−5910	0.81420	9	9	18	290.69	4322.4
0.5034	220−350	490−5330	0.62627	7	7	14	284.89	3514.0
0.6199	220−360	370−6050	0.73056	8	8	16	292.05	3928.4
0.7920	220−360	340−5650	0.68917	8	7	15	292.82	3679.3

[a] 2ph and vap denote data within the VLE boundary and superheated region, respectively.

Table 2. Experimental Data within the VLE Boundary for the R116 (1) + CO_2 (2) System

x_1	T/K	P/kPa	V/m^3·mol^{-1}	x_1	T/K	P/kPa	V/m^3·mol^{-1}
0.2022					227.33	853.7	0.932
	214.17	561.6	0.419		232.37	1000.5	0.932
	217.21	635.2	0.419		237.46	1162.6	0.933
	222.28	775.1	0.420		242.53	1336.5	0.933
	232.40	1118.9	0.420		247.60	1524.9	0.933
	237.47	1328.9	0.420				
	242.54	1566.9	0.420	0.6396			
	247.61	1835.0	0.420		214.18	477.2	1.187
	252.69	2133.4	0.420		217.20	529.7	1.188
0.3964					222.25	626.3	1.188
	214.17	556.5	0.822		227.33	735.0	1.188
	217.19	625.1	0.822		232.39	854.1	1.188
	222.25	756.3	0.823		237.45	985.9	1.189
	227.31	907.9	0.823		242.56	1132.8	1.189
	232.37	1075.7	0.823	0.7702			
	237.40	1259.0	0.823		214.18	398.4	1.430
	242.51	1461.1	0.823		217.21	442.4	1.430
	247.60	1654.9	0.823		222.26	523.5	1.430
0.5019					227.34	615.9	1.431
	214.16	535.1	0.932		232.38	720.3	1.431
	217.20	599.8	0.932		237.48	837.2	1.431
	222.26	719.4	0.932		242.56	968.1	1.432

Table 3. Experimental Data within the VLE Boundary for the R41 (1) + CO_2 (2) System

x_1	T/K	P/kPa	V/m^3·mol^{-1}	x_1	T/K	P/kPa	V/m^3·mol^{-1}
0.2431					252.70	1466.4	0.436
	222.30	574.4	0.802		262.90	1984.9	0.436
	227.35	701.7	0.802		273.06	2617.7	0.436
	232.41	848.1	0.803		283.36	3344.8	0.437
	237.47	1017.8	0.803	0.6199			
	242.55	1209.3	0.803		217.23	369.6	0.373
	247.60	1425.6	0.803		227.32	562.9	0.373
	252.70	1666.6	0.803		237.42	823.9	0.374
	257.88	1917.4	0.804		247.56	1167.0	0.374
0.3919					257.82	1610.3	0.374
	222.29	529.7	0.335		268.02	2156.4	0.374
	227.35	649.5	0.335		278.06	2813.5	0.374
	232.40	787.1	0.335		288.43	3609.9	0.374
	237.48	947.9	0.335	0.7920			
	242.53	1128.9	0.335		217.25	335.0	0.396
	252.71	1571.1	0.335		227.33	509.9	0.396
	262.89	2127.3	0.336		237.45	746.5	0.396
	273.11	2810.0	0.336		247.59	1059.2	0.396
	283.37	3638.9	0.336		257.59	1461.3	0.396
0.5034					267.97	1961.6	0.397
	222.27	492.2	0.436		278.06	2572.0	0.397
	232.35	732.4	0.436		288.42	3320.8	0.397
	242.55	1054.9	0.436				

able. Then, from the solution of the two equations representing the system's behavior in the two-phase and superheated regions, the temperature and pressure corresponding to the dew point were found algebraically for each isochore. The solutions are given in Table 1.

VLE Derivation. Two methods were used to derive VLE data from the isochoric measurements, as described elsewhere.[4]

In the first, the VLE parameters were derived using the dew-point method with the CSD EOS. The necessary dew-point parameters (Table 1) were used as independent variables, whereas the interaction binary parameter K_{12} and the corresponding pressure and liquid-phase composition at the bubble point (considered to be dependent variables) were adjusted until the phase equilibrium condition was reached. The resulting K_{12} values and bubble-point parameters are shown in Table 6. In the second method, the VLE parameters were derived for each data point in the two-phase region using the flash method with the CSD EOS. To apply the flash method to isochoric data, the volumetric properties of both phases are also needed and were calculated from the CSD EOS. During the fitting procedure, T, P, zi and n (number of moles charged) were kept constant for each experimental point. Because the isochoric cell volume was known from the gravimetric calibration, the binary interaction parameter K_{12} and the compositions at the bubble and dew points were found and were considered to be dependent variables. The K_{12} values found for each data point in the two-phase region are shown in Figures 2 and 3 for R116 + CO_2 and R41 + CO_2, respectively.

Table 4. Experimental Data in the Superheated Vapor Region for the R116 (1) + CO_2 (2) System

x_1	T/K	P/kPa	V/m^3·mol^{-1}	x_1	T/K	P/kPa	V/m^3·mol^{-1}
0.2022					324.14	2481.6	0.936
	262.88	2841.3	0.420		334.34	2590.1	0.937
	273.10	3451.2	0.420		344.53	2695.7	0.937
	283.34	3746.0	0.421		354.75	2801.7	0.937
	295.56	4081.4	0.421	0.6396			
	303.73	4301.8	0.421		247.60	1289.7	1.189
	313.90	4571.4	0.421		252.72	1362.7	1.189
	324.15	4835.3	0.421		262.88	1465.1	1.190
	334.36	5100.0	0.422		273.09	1554.9	1.191
	344.56	5358.2	0.422		283.00	1640.6	1.191
	354.77	5614.0	0.422		294.51	1737.4	1.192
0.3964					303.71	1815.9	1.192
	252.69	1811.7	0.824		313.88	1900.1	1.193
	262.89	2002.6	0.824		324.15	1983.2	1.193
	273.09	2159.2	0.824		334.35	2066.0	1.194
	283.34	2292.1	0.825		344.56	2148.3	1.194
	294.51	2429.4	0.825		354.76	2230.0	1.195
	303.67	2548.2	0.825	0.7702			
	313.89	2673.6	0.826		247.63	1095.9	1.432
	324.16	2798.4	0.826		252.71	1155.5	1.432
	334.35	2922.1	0.827		257.83	1200.3	1.433
	344.56	3042.9	0.827		262.88	1237.3	1.433
	354.75	3163.6	0.827		272.90	1309.5	1.434
0.5019					283.35	1383.5	1.434
	252.66	1670.6	0.933		294.58	1461.6	1.435
	262.82	1805.9	0.934		303.72	1524.3	1.436
	273.03	1923.8	0.934		313.90	1593.4	1.436
	282.98	2035.7	0.935		324.16	1662.5	1.437
	294.50	2163.5	0.935		334.36	1730.8	1.437
	303.67	2263.1	0.935		344.56	1798.4	1.438
	313.82	2371.9	0.936		354.76	1865.8	1.439

Table 5. Experimental Data in the Superheated Vapor Region for the R41 (1) + CO_2 (2) System

x_1	T/K	P/kPa	V/m^3·mol^{-1}	x_1	T/K	P/kPa	V/m^3·mol^{-1}
0.2431					313.85	4299.9	0.437
	262.96	2084.7	0.804		324.14	4567.5	0.437
	273.12	2243.3	0.804		334.33	4825.7	0.438
	283.37	2378.2	0.804		344.56	5080.8	0.438
	298.63	2572.6	0.805		354.75	5330.9	0.438
	308.81	2699.0	0.805	0.6199			
	318.99	2823.7	0.806		298.59	4144.1	0.375
	329.26	2947.8	0.806		303.69	4313.3	0.375
	339.46	3069.5	0.806		313.36	4648.0	0.375
0.3919					324.16	4971.9	0.375
	293.53	4400.8	0.336		334.36	5287.4	0.375
	298.64	4625.1	0.336		344.57	5596.5	0.375
	303.72	4817.1	0.336		354.77	5900.8	0.376
	308.75	5003.5	0.336		359.87	6050.9	0.376
	313.92	5191.6	0.336	0.7920			
	318.96	5372.0	0.336		298.60	3859.1	0.397
	324.16	5556.4	0.336		308.77	4175.6	0.397
	329.26	5734.8	0.337		319.06	4486.0	0.397
	334.37	5911.5	0.337		329.26	4785.6	0.398
0.5034					339.46	5078.7	0.398
	293.52	3752.0	0.437		349.67	5366.9	0.398
	303.68	4029.2	0.437		359.87	5650.0	0.398

Table 6. Binary Interaction Parameters and Bubble-Point Composition (x_1) Found from the Dew Point by Applying the CSD EOS

R116 (1) + CO_2 (2)					R41 (1) + CO_2 (2)				
series	K_{12dew}	$K_{12flash}$	$K'_{12flash}$[a]	x_1	series	K_{12dew}	$K_{12flash}$	$K'_{12flash}$[a]	x_1
1	0.0615	0.0647	0.0792	0.2203	1	−0.0026	−0.0049	−0.0097	0.3257
2	0.0631	0.0722	0.0772	0.5168	2	0.0009	−0.0054	−0.0080	0.4603
3	0.0767	0.0812	0.0793	0.6773	3	−0.0023	−0.0068	−0.0081	0.5814
4	0.0759	0.0901	0.0798	0.8091	4	−0.0053	−0.0086	−0.0079	0.6839
5	0.0696	0.0979	0.0812	0.8942	5	−0.0085	−0.0104	−0.0061	0.8348
av	0.0694	0.0819	0.0794		av	−0.0035	−0.0072	−0.0078	

[a] Values of $K'_{12flash}$ were obtained with $L_{12} = -0.025$ and 0.0077 for R116 + CO_2 and R41 + CO_2, respectively.

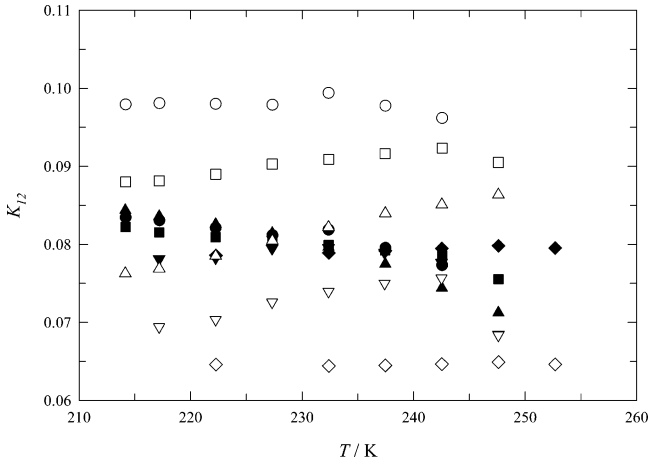

Figure 2. K_{12} values found by the flash method for the R116 + CO_2 system: solid symbols, K_{12} values found with the Adachi and Sugie[15] mixing rule with $L_{12} = -0.025$.

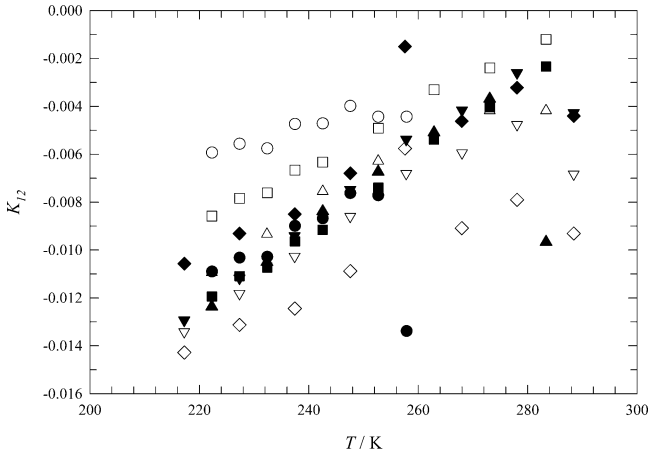

Figure 3. K_{12} values found by the flash method for the R41 + CO_2 system: solid symbols, K_{12} values found with the Adachi and Sugie[15] mixing rule with $L_{12} = -0.0077$.

In another attempt to assess the quality of the derived VLE parameters, the system pressure was reproduced using the averaged K_{12} values. The pressure deviations are plotted in Figures 4 and 5 for the R116 + CO_2 and R41 + CO_2 systems, respectively. Analyzing the pressure deviations (Figure 4) suggests that the R116 + CO_2 system is not quite symmetrical in terms of the 1-vdW mixing rule applied. This becomes even more evident when the K_{12} values obtained are plotted against the liquid-phase composition (Figure 6). These results would prompt the use of a composition-dependent mixing rule, the choice of which is limited when the CSD EOS is applied. Brandani and Brandani[10] have already proven that very popular mixing rules through the g^E at infinite pressures (such as those proposed by Huron and Vidal[11] and Wong and Sandler[12])

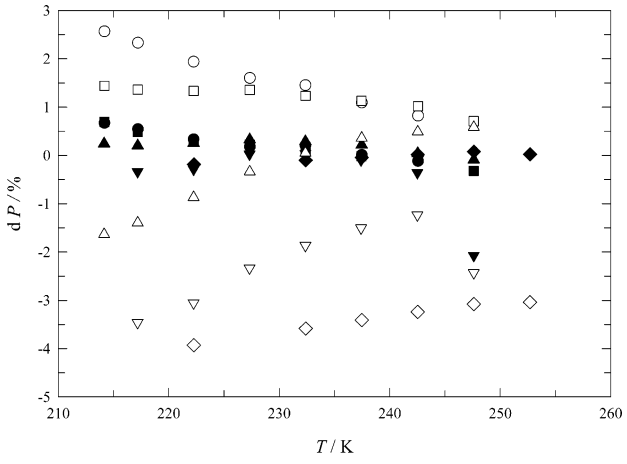

Figure 4. Pressure deviations, $dP\% = 100(P_{exptl} - P_{calcd})/P_{exptl}$, between experimental values and those calculated with the K_{12} coefficients for the R116 + CO_2 system: solid symbols, K_{12} values found with $L_{12} = -0.025$.

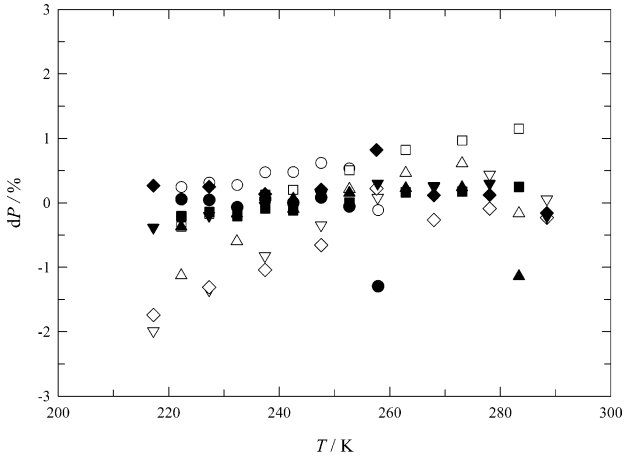

Figure 5. Pressure deviations, $dP\% = 100(P_{exptl} - P_{calcd})/P_{exptl}$, between experimental values and those calculated with the K_{12} coefficients for the R41 + CO_2 system: solid symbols, K_{12} values found with $L_{12} = -0.0077$.

that have been successfully applied to the cubic EOS are inappropriate for EOSs with hard-sphere models in the repulsive term, such as the CSD. The composition-dependent mixing rule can, however, be imposed directly in the mixing rule for the a parameter. Such composition-dependent mixing rules were proposed in 1984 for the cubic EOS by Panagiotopoulos and Reid,[13] Stryjek and Vera,[14] and Adachi and Sugie,[15] all with two adjustable parameters, and were later made even more flexible, with up to three adjustable parameters, by Schwartzentruber and Renon.[16] In fact, after their algebraic transformation, all of these mixing rules are equivalent for binary systems. For the

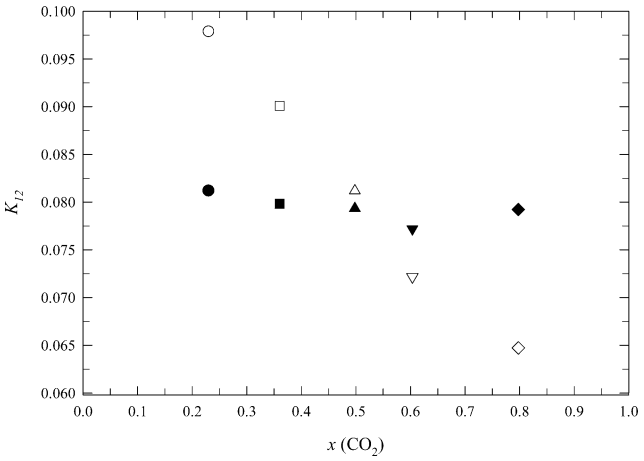

Figure 6. Averaged K_{12} coefficients for the R116 + CO_2 system obtained with $L_{12} = 0$ (open symbols) and $L_{12} = -0.025$ (solid symbols).

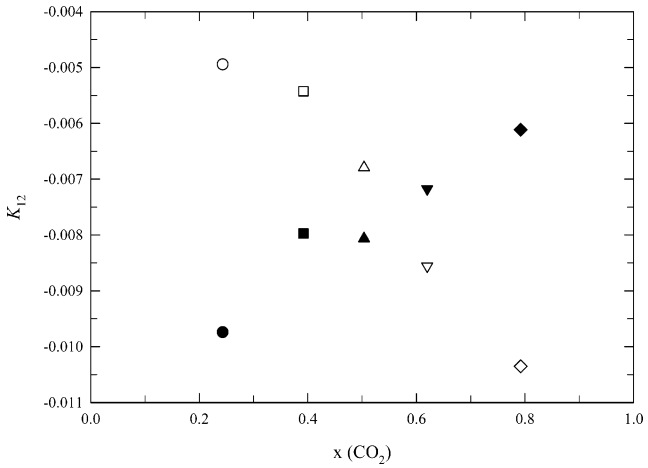

Figure 7. Averaged K_{12} coefficients for the R41 + CO_2 system obtained with $L_{12} = 0$ (open symbols) and $L_{12} = -0.0077$ (solid symbols).

reader's convenience, we used the Adachi−Sugie, which is identical to the Schwartzentruber−Renon, form:

$$a_{ij} = (a_{ii}a_{jj})^{1/2}[1 - k_{ij} - l_{ij}(x_i - x_j)] \qquad (1)$$

In this formalism, the second adjustable parameter ($l_{ij} = -l_{ji}$), contrary to classical $k_{ij} = k_{ji}$, is clearly distinguished, whereas $k_{ij} \neq k_{ji}$ in the first two of the above-mentioned mixing rules.

Another difficulty arises from using models with two (or more) adjustable parameters when the VLE parameters are derived from isochoric data. In the method that we used before, each experimental $P-T$ datum set was correlated individually, and then the resulting K_{12} values were averaged, assuming that their equal statistical weight and the resulting average values were used to calculate the pressure deviations from the fit. Applying the composition-dependent mixing rule, however, we first assumed the temperature independence of the K_{12}, and two parameters were found from the simultaneous correlation of all data belonging to the two-phase region. Analyzing the fitting results, we found that the pressure deviations are randomly distributed in relation to both composition and temperature, thus confirming that the model with two adjustable temperature-independent parameters can represent the experimental data more accurately. The results obtained with the Adachi−Sugie mixing rule are given in Figures 2 to 7 using black symbols. Fitting results are also shown in Table 6. It is worth noting that adopting $l_{12} = -0.025$ for R116 + CO2 and $l_{12} = 0.0077$ for R41 + CO_2 induced a clear reduction in the pressure deviation, as shown in Figures 4 and 5.

Using the parameters found for the two mixing rules, we calculated the VLE data for three temperatures to gain an impression of the system's properties. The results are given in Figures 8 and 9. Figure 8 shows that the system has a strong positive deviation from Raoult's law, with an azeotrope at about $x_{az} = 0.20$ at $T = 253.15$ K and $P = 2202.33$ kPa. Figure 8 also shows data from the literature, obtained at $T = 227.6$ K,[5] as open circles, whereas the present measurements were regressed at the same temperature and shown as a solid line. The comparison shows satisfactory consistency between the two sources of data. Figure 9 shows that the R41 + CO_2 system has almost ideal behavior in terms of Raoult's law. To compare the present results with the literature, we correlated the Outcalt et al.[6] VLE data with the CSD EOS and found the average $k_{12} = -0.0059$. This reproduces their data with an absolute average deviation in d$P\% = 0.73$. The comparison with our data was made at $x = 0.50$ and $T = 253.15$ K and showed a deviation of d$P\% = 100(P_{flash} - P_{NIST})/P_{flash} = -0.32\%$. That agreement can be considered satisfactory. Finally, g^E values were calculated for the two systems and

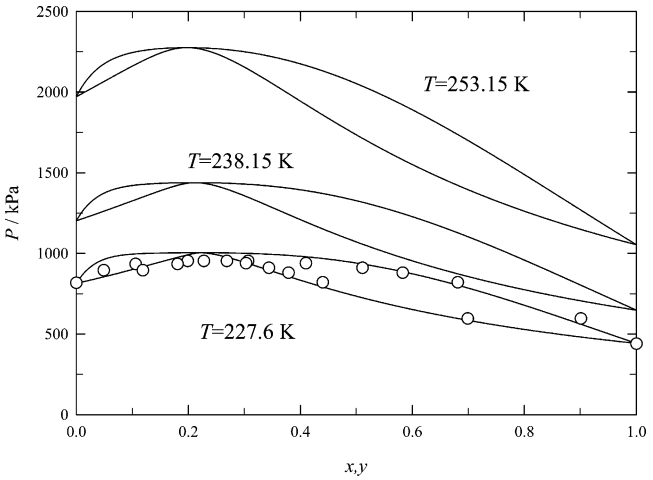

Figure 8. VLE representation from the correlation with eq 1 for the R116 + CO_2 system at three temperatures; O, experimental data from Shiflets and Sandler.[5]

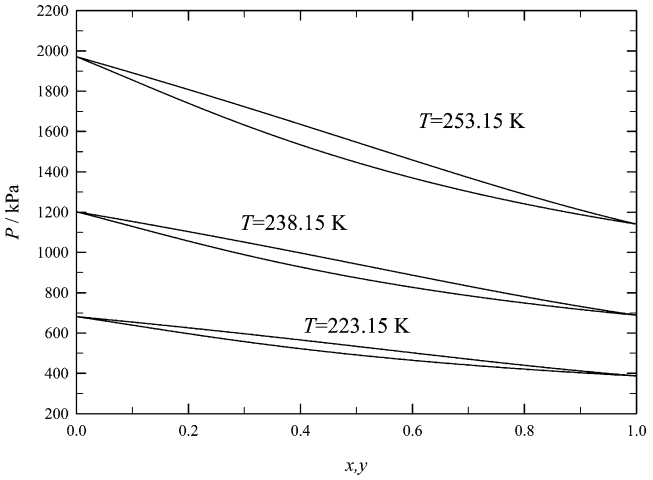

Figure 9. VLE representation from the correlation with eq 1 for the R41 + CO_2 system at three temperatures.

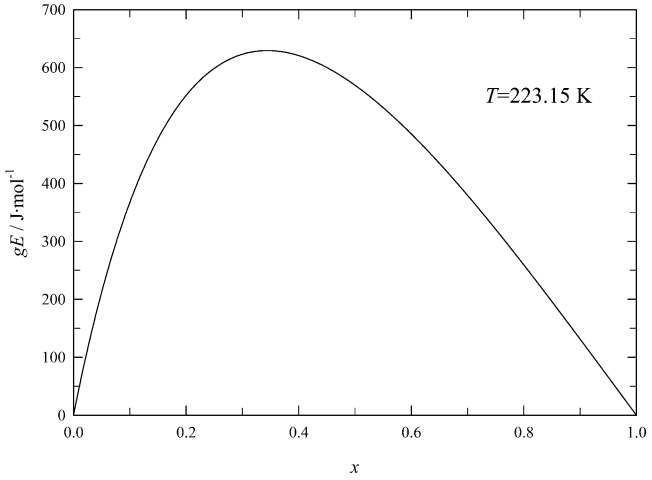

Figure 10. Excess Gibbs function for the R116 + CO_2 system at T = 223.15 K.

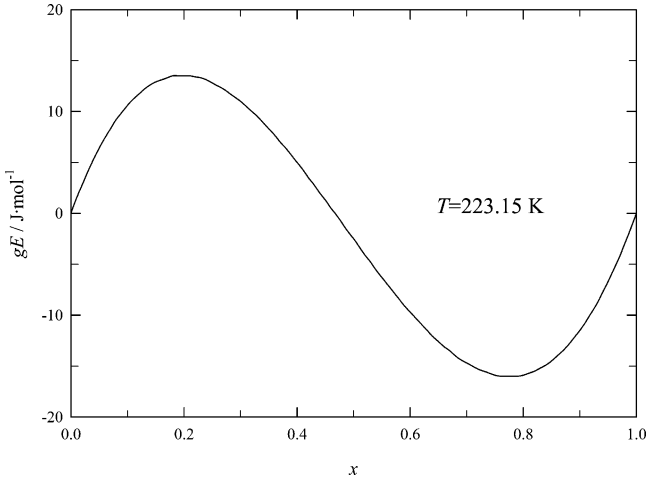

Figure 11. Excess Gibbs function for the R41 + CO_2 system at T = 223.15 K.

plotted versus the liquid-phase composition in Figures 10 and 11. An S-shaped behavior of g^E is clearly evident for R41 + CO_2, although the g^E values are very small and change sign. For R116 + CO_2, the g^E values are strongly positive, and $g^E(x)$ is asymmetrical.

PVTx. Our experimental *PVTx* data were compared with the REFPROP 7[17] estimates, as shown in Figures 12 and 13. The average absolute pressure deviation was 0.29% and 0.53% for R116 + CO_2 and R41 + CO_2, respectively.

The experimental *PVTx* data obtained from the isochoric measurements and those calculated by applying the virial EOS with coefficients found from the Burnett experiment[18,19] were also compared. The results are shown in Figures 14 and 15. Data within the two vertical lines were obtained in the same temperature range as the Burnett data. For the R116 + CO_2 system, there was good consistency over whole temperature range, the deviations being within ±1% (with the exception of a few points). For the R41 + CO_2 system, deviations average around 1% for temperatures T < 343 K, but a systematic deviation is observed for temperatures T > 343 K, which increases to 3 to 4% at the highest temperatures. This greater deviation with rising temperatures is presumably due to (i) the extrapolation of the virial coefficients for higher temperatures using purely empirical expressions for their temperature dependence and (ii) the relatively short temperature range covered by the Burnett experiment. The global

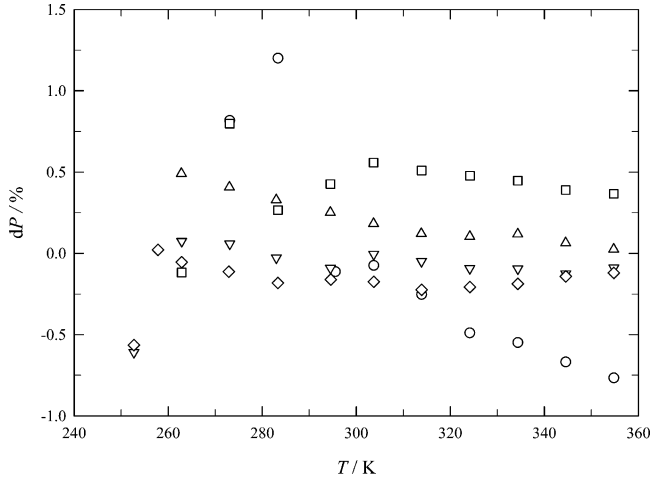

Figure 12. Pressure deviations for the R116 + CO_2 system between experimental values and those calculated with the REFPROP 7 estimate.

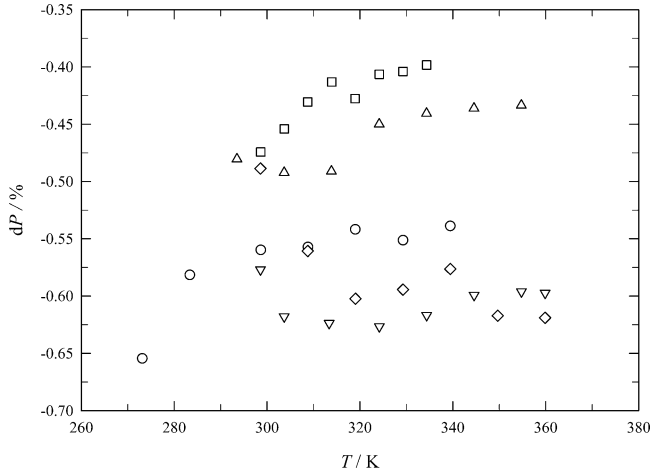

Figure 13. Pressure deviations, $dP\% = 100(P_{exptl} - P_{calcd})/P_{exptl}$, for the R41 + CO_2 system between experimental values and those calculated with the REFPROP 7 estimate.

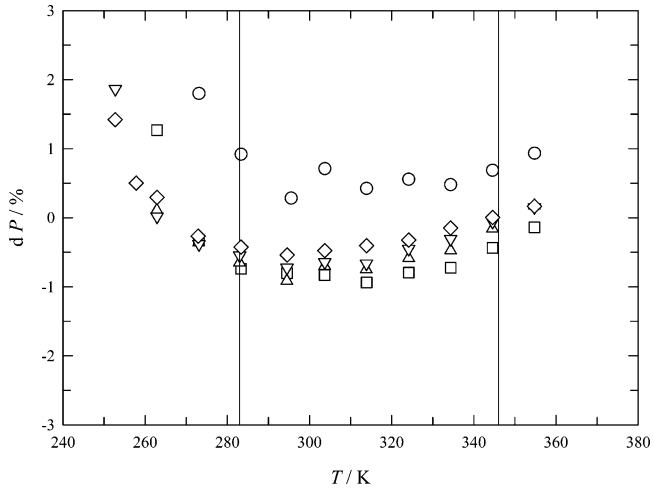

Figure 14. Pressure deviations, $dP\% = 100(P_{exptl} - P_{calcd})/P_{exptl}$, for the R116 + CO_2 system between experimental values from isochoric and Burnett results.[18] The vertical lines correspond to the minimum and maximum temperatures of the Burnett measurements.

consistency between the data obtained can be considered satisfactory, however, and well within the experimental uncertainties of the two different methods.

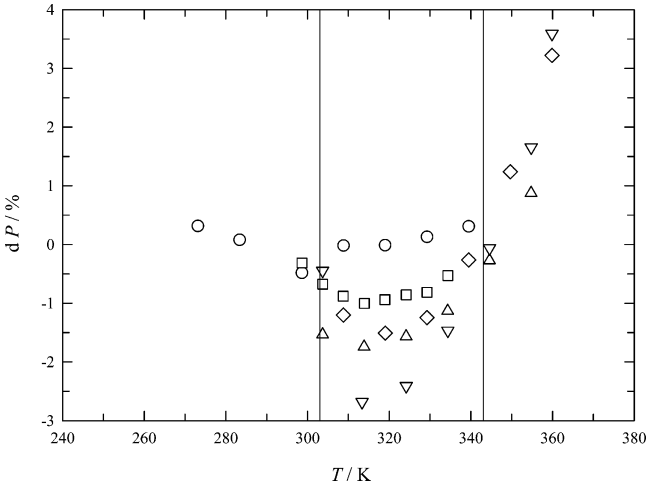

Figure 15. Pressure deviations, $dP\% = 100(P_{exptl} - P_{calcd})/P_{exptl}$, for the R41 + CO_2 system between experimental values from isochoric and Burnett results.[19] The vertical lines correspond to the minimum and maximum temperatures of the Burnett measurements.

Conclusions

A new isochoric apparatus was used for *PVTx* measurements on the R116 + CO_2 and R41 + CO_2 systems. The binary interaction parameters were derived from experimental data in the two-phase region by applying the flash method and the Carnahan−Starling−DeSantis equation of state (CSD EOS). The dew-point parameters were found by interpolating the $P-T$ isochoric sequences, again applying the CSD EOS. The binary interaction parameters were calculated by adopting both the van der Waals and the Adachi−Sugie mixing rules. The calculated binary interaction parameters were used to derive the VLE parameters. The R116 + CO_2 system showed a strong positive deviation from Raoult's law, with an azeotrope, whereas the R41 + CO_2 system showed almost ideal behavior in terms of Raoult's law.

Independent experiments using both the Burnett and the isochoric setups enabled us to check the internal consistency of all of the results. The values emerging from our experimental density data in the superheated region were also compared with data calculated using the REFPROP 7 program, and a consistency to within 0.5% was recorded. This also validates the cross virial coefficients derived using the Burnett method. Generally speaking, the global validity of the methods and results can be claimed to within 1% of the density and/or pressure values.

Acknowledgment

This work was supported by MIUR, Ministry of Instruction, University and Research, and by the government of the Marche region.

Literature Cited

(1) Di Nicola, G.; Pacetti, M.; Polonara, F.; Stryjek, R. Isochoric Measurements for CO_2 + R125 and CO_2 + R32 Binary Systems. *J. Chem. Eng. Data* **2002**, *47*, 1145−1153.
(2) Di Nicola, G.; Giuliani, G.; Polonara, F.; Stryjek, R. Isochoric Measurements for R23 + CO_2 Binary System. *Fluid Phase Equilib*. **2003**, *210*, 33−43.
(3) De Santis, R.; Gironi, F.; Marrelli, L. Vapor-Liquid Equilibrium from a Hard-Sphere Equation of State. *Ind. Eng. Chem. Fundam*. **1976**, *15*, 183−189.
(4) Di Nicola, G.; Giuliani, G.; Passerini, G.; Polonara, F.; Stryjek, R. Vapor-Liquid Equilibria (VLE) Properties of R-32 + R-134a System Derived from Isochoric Measurements. *Fluid Phase Equilib*. **1998**, *153*, 143−165.
(5) Shiflets, M. B.; Sandler, S. I. Modelling Fluorocarbon Vapor-Liquid Equilibria Using the Wong-Sandler Model. *Fluid Phase Equilib*. **1998**, *147*, 145−162.
(6) Outcalt, C. D.; Magee, J. W.; Scott, J. L.; Outcalt, S. L.; Haynes, W. M. Selected Thermodynamic Properties for Mixtures of R-32 (Difluoromethane), R-134A (1,1,1,2-Tetrafluoroethane), R143A (1,1,1-Trifluoroethane), R-41 (Fluoromethane), R-290 (Propane), and R-744 (Carbon Dioxide). NIST Technical Note 1397; National Institute of Standards and Technology: Boulder, CO, 1997.
(7) Giuliani, G.; Kumar, S.; Zazzini, P.; Polonara, F. Vapor Pressure and Gas Phase PVT Data and Correlation for 1,1,1,-Trifluoroethane (R143a). *J. Chem. Eng. Data* **1995**, *40*, 903−908.
(8) Giuliani, G.; Kumar, S.; Polonara, F. A Constant Volume Apparatus for Vapour Pressure and Gas Phase *P-v-T* Measurements: Validation with Data for R22 and R134a. *Fluid Phase Equilib*. **1995**, *109*, 265−279.
(9) Di Nicola, G.; Polonara, F.; Stryjek, R. $P-V-T-x$ and Vapor−Liquid Equilibrium Properties of Pentafluoroethane (R125) + 1,1,1,3,3,3-Hexafluoroethane (R236fa) and 1,1,1,2-Tetrafluoroethane (R134a) + (R236fa) Systems Derived from Isochoric Measurements. *J. Chem. Eng. Data* **2001**, *46*, 359−366.
(10) Brandani, S.; Brandani, V. On the Inapplicability of Mixing Rules Based on the Infinite Pressure Reference State for Equations of State Which Use the Hard-Sphere Repulsive Term. *Fluid Phase Equilib*. **1996**, *121*, 179−184.
(11) Huron, M. J.; Vidal, J. New Mixing Rules in Simple Equations of State for Representing Vapour-Liquid Equilibria of Strongly Non-Ideal Mixtures. *Fluid Phase Equilib*. **1979**, *3*, 255−271.
(12) Wong, D. S. H.; Sandler, S. I. A Theoretically Correct Mixing Rule for Cubic Equations of State. *AIChE J*. **1992**, *38*, 671−680.
(13) Panagiotopoulos, A. Z.; Reid, R. C. New Mixing Rule for Cubic Equations of State for Highly Polar, Asymmetric Systems. *ACS Symp. Ser*. **1986**, *300*, 571−582.
(14) Stryjek, R.; Vera, J. H. PRSV2: A Cubic Equation of State for Accurate Vapor-Liquid Equilibria Calculations. *Can. J. Chem. Eng*. **1986**, *64*, 820−826.
(15) Adachi, Y.; Sugie, H. A New Mixing Rule − Modified Conventional Mixing Rule. *Fluid Phase Equilib*. **1986**, *28*, 103−118.
(16) Schwartzentruber, J.; Renon, H. Extension of UNIFAC to High Pressures and Temperatures by the Use of a Cubic Equation of State. *Ind. Eng. Chem. Res*. **1989**, *28*, 1049−1055.
(17) Lemmon, E. W.; McLinden, M. O.; Huber, M. L. NIST Standard Reference Database 23, NIST Thermodynamic Properties of Refrigerants and Refrigerant Mixtures Database (REFPROP), version 7.0; National Institute of Standards and Technology: Gaithersburg, MD, 2002.
(18) Di Nicola, G.; Giuliani, G.; Passerini, G.; Polonara, F.; Stryjek, R. Virial Coefficients from Burnett Measurements for the R116 + CO_2 System. *Int. J. Thermophys*. **2004**, *25*, 1437−1447.
(19) D'Amore, A.; Di Nicola, G.; Polonara, F.; Stryjek, R. Virial Coefficients from Burnett Measurements for the Carbon Dioxide + Fluoromethane System. *J. Chem. Eng. Data* **2003**, *48*, 440−444.

Received for review February 6, 2004. Accepted December 15, 2004.

JE049939G